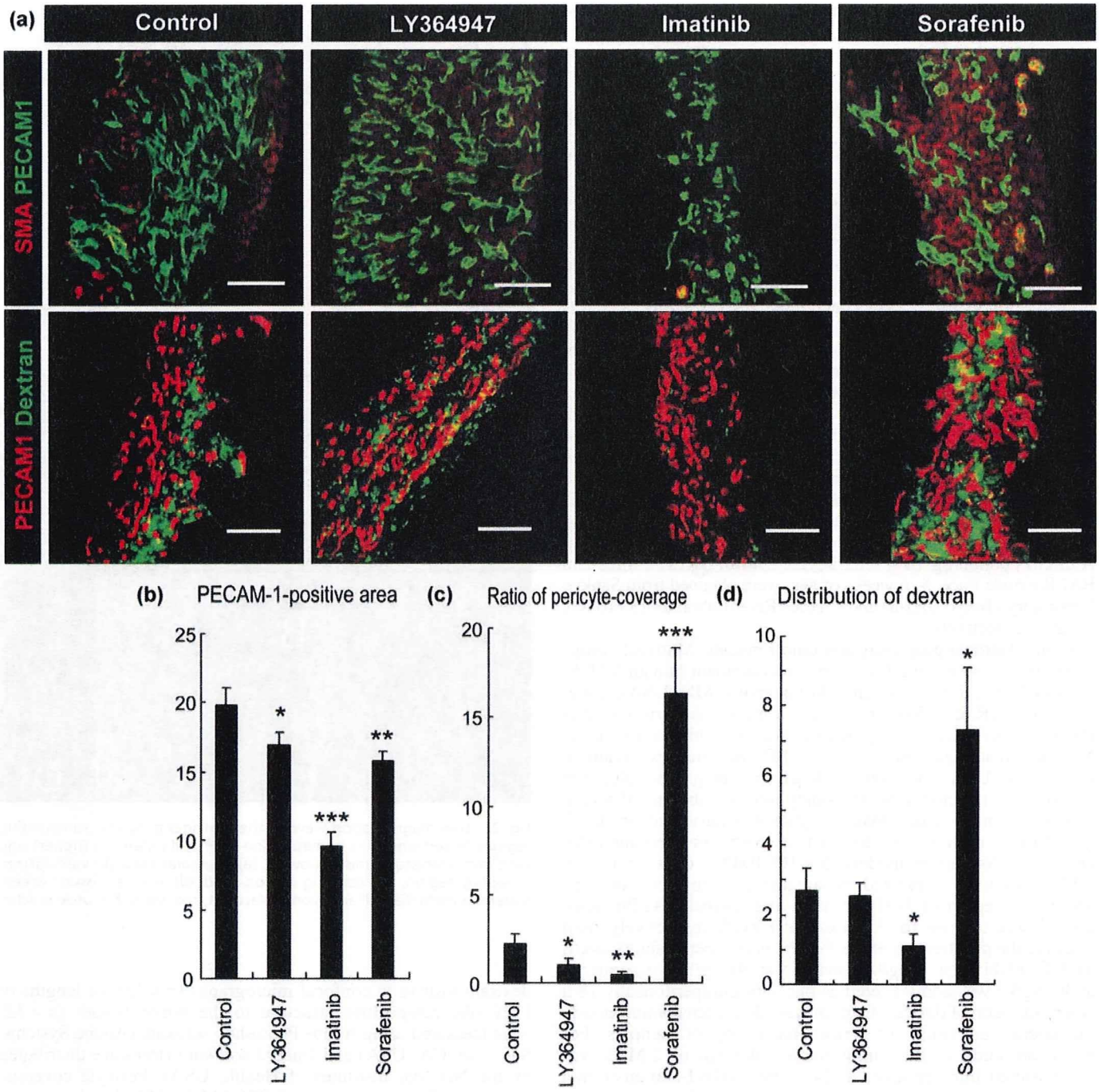

Fig. 3. Effects of three types of kinase inhibitors on extravasation of dextran from vasculature in the periplug region. (a) Confocal microscopy analyses. Upper row: staining of platelet endothelial cell adhesion molecule (PECAM)-1-positive endothelium in green and smooth muscle α-actin (SMA)-positive pericytes in red. Lower row: distribution of 2 MDa dextran in green and PECAM-1-positive endothelium in red. Scale bars = 100 μm. (b–d) Results of quantification (n = 15) of areas of endothelium (b, in percentage in one microscopic view), ratio of pericyte-covered endothelium (c, in percentage), and dextran distribution (d, in percentage in one microscopic view). Bars in the graphs represent standard errors. *P < 0.05; **P < 0.01; and ***P < 0.001.

with our previous study, in which we used animal models of pancreatic adenocarcinoma and diffuse-type gastric cancer.[7] Based on this result, we expected that a decrease in pericytes might induce more extravasation of 2 MDa dextran.

To confirm this, we compared the effects of imatinib administration, which inhibits PDGF signaling and may therefore decrease pericyte coverage. However, administration of imatinib decreased the total accumulation of 2 MDa dextran compared with TGF-β inhibitor (Fig. 1). Although imatinib actually decreased pericyte coverage to the same level of TGF-β inhibitor, it also decreased PECAM-1-positive endothelium together with pericyte coverage. These findings of morphological analysis were consistent with those noted in a previous report.[17] TGF-β inhibitor maintained the area of PECAM-1-positive endothelium and may therefore be superior to imatinib. In addition, although VEGF inhibition was expected to increase drug delivery, based on the

doi: 10.1111/j.1349-7006.2008.01003.x

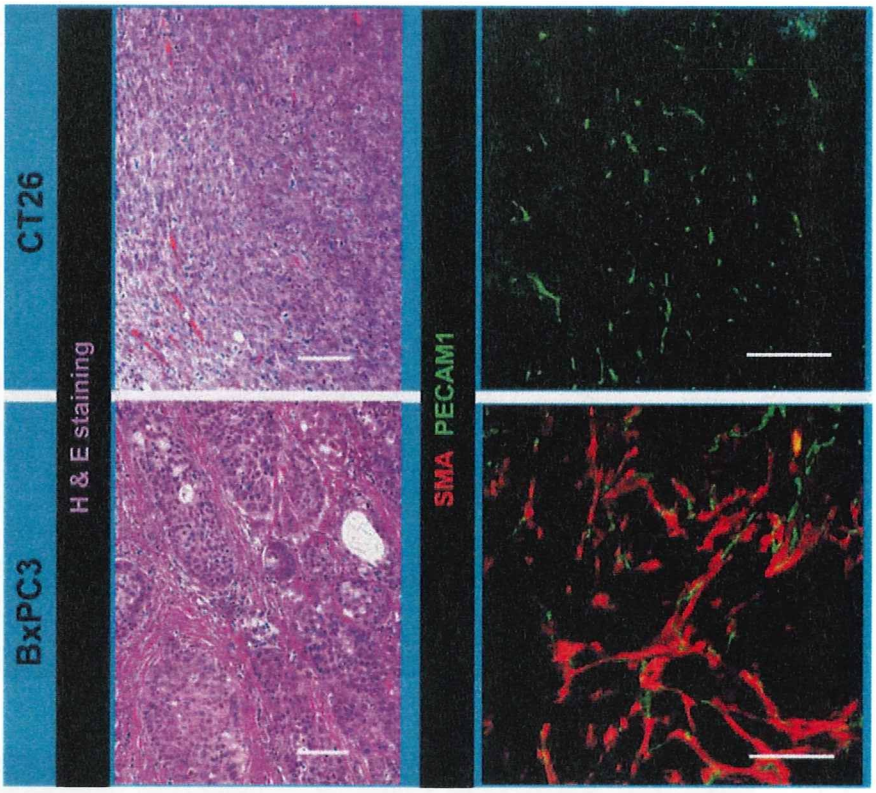

Fig. 4. Two animal tumor models using CT26 and BxPC3 cell lines. Histological examination of tumor models by hematoxylin–eosin staining and immunohistochemistry with platelet endothelial cell adhesion molecule (PECAM)-1 in green and smooth muscle α-actin (SMA) in red. Scale bars = 100 μm.

results of previous studies,[8] sorafenib nearly eliminated the influx of 2 MDa dextran and resulted in far less accumulation of it. This result can be explained by the potent reduction of PECAM-1-positive endothelium and increase in pericytes as sleeves. These morphological changes induced by VEGF inhibition were also consistent with previous reports.[18]

Although the neovasculature inside the gel plugs was as described above, the vasculature in the regions surrounding the gel plugs, or sites of acute inflammation in reaction to the plugs as foreign bodies (Fig. 2), exhibited different patterns. Compared to the vasculature inside the gel plug, that in regions around the plugs was denser and more tortuous, and was accompanied by pericytes to a smaller extent. These phenotypes resembled those of the vasculature in conventional animal models of tumors, such as the CT26 model, as we describe later in this report. We termed these two regions the 'intraplug' and 'periplug' regions, respectively, after the established terminology in oncology, 'intratumoral' and 'peritumoral'.

Functionally, the vasculature in periplug regions was leaky to 2 MDa dextran in the control condition, that is, without any modulation by SMWI (Fig. 3). Surprisingly, the effects of SMWI on neovasculature in the periplug regions were quite different from those in the intraplug regions. In the periplug regions, pericyte coverage of the neovasculature was far less than in the intraplug region, even in the control condition. In this periplug region, neither TGF-β inhibitor nor imatinib significantly altered pericyte coverage. Consequently, these compounds did not alter the accumulation of 2 MDa dextran. Sorafenib, on the other hand, did increase pericyte coverage, and increased the accumulation of 2 MDa dextran. This increase in extravasation was consistent with previous reports on the effects of VEGF inhibition.[8]

We subsequently compared these findings in the Matrigel plug assay with those in two subcutaneous tumor xenograft models. We used the CT26 cell line derived from murine colon cancer and the BxPC3 cell line derived from human pancreatic adenocarcinoma (Fig. 4). HE staining of CT26 xenografts revealed a well-vascularized medullary histological pattern with little tumor stroma, whereas that of BxPC3 xenografts revealed a stroma-rich histology. Immunostaining of PECAM-1 and SMA confirmed this stroma-rich characteristic of the BxPC3 model. Although the BxPC3 model grew more slowly than the CT26 model, the BxPC3 model also reached the proliferative phase. Compared to the BxPC3 model, the CT26 model required one-fifth of the number of inoculating cells and one-third of the duration to reach the proliferative phase, which was 1 week for the CT26 model and 3 weeks for the BxPC3 model (data not shown). These differences may well be due to the differences in requirements for induction of stromal components from host animals, as well as rates of proliferation of tumor cell lines.

We then tested the alterations in vascular phenotypes as well as accumulation of 2 MDa dextran with or without SMWI in these tumor models (Fig. 5). We here used NG2 as the pericyte marker (Fig. 5a), because SMA-positive cells (i.e. myofibroblasts) are abundant especially in the stroma of BxPC3 tumor (Fig. 4). In the CT26 model, sorafenib did increase the pericyte-covered vasculature, whereas other SMWI did not increase the pericytes. Imatinib decreased endothelial cells. These observations in the CT26 tumor model were consistent with those in the periplug region of the Matrigel plug. In the BxPC3 model, pericyte coverage was less with LY364947 and imatinib, and endothelial cells were decreased with imatinib and sorafenib. These findings in the BxPC3 tumor model were consistent with those in the intraplug region. Accordingly, 2 MDa dextran was diffusely distributed in tumor tissue without any treatment in the CT26 model, whereas almost no leakage of dextran was observed in the BxPC3 model (Fig. 5b). Sorafenib exhibited the best effect in the CT26 model, whereas TGF-β inhibitor did in the BxPC3 model. The latter result was consistent with the findings of our previous work using nanoparticles including PEGylated liposomes incorporating doxorubicin (Doxil) of approximately 100 nm in diameter, which exhibited antitumor effects in the BxPC3 model

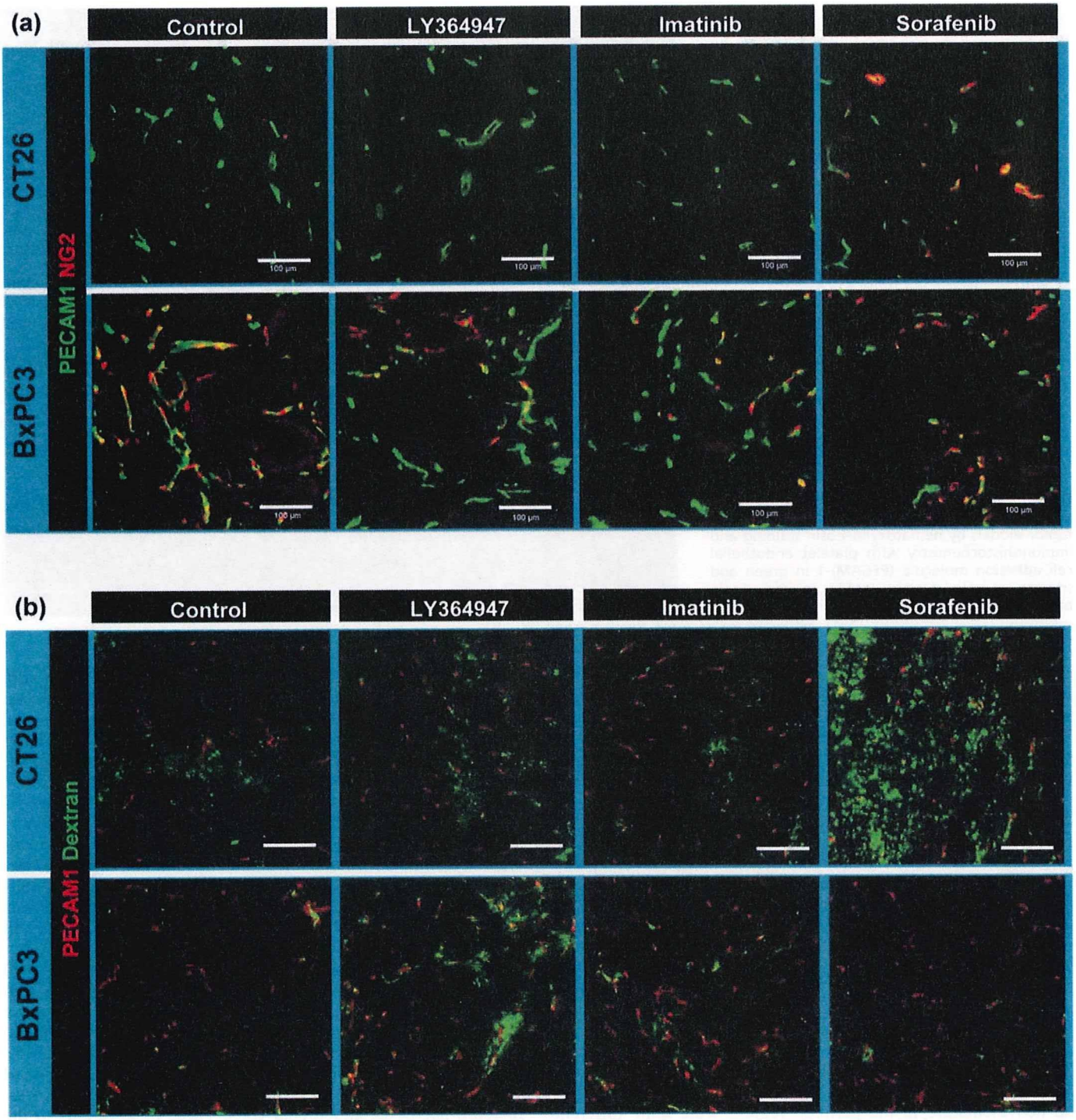

Fig. 5. Effects of three kinase inhibitors in the tumor models. (a) Vascular phenotypes revealed by immunohistochemistry. Green, platelet endothelial cell adhesion molecule (PECAM)-1; red, NG2. (b) Extravasation of 2 MDa dextran from vasculature. Dextran in green and PECAM-1 in red. Scale bars = 100 μm.

only when combined with TGF-β inhibitor.[7] We also tested the effects of Doxil with or without TGF-β inhibitor in the CT26 model. Monotherapy with Doxil at 8 mg/kg almost completely inhibited tumor growth, and combined administration of TGF-β inhibitor did not yield any significant additional effects (data not shown). These findings were consistent with those observed in the Matrigel plug assay. The effects of combined use of imatinib were also consistent with those in the Matrigel plug assay.

Increased accumulation of dextran in these tumor models at 7 h after injection, by sorafenib in the CT26 tumor and by LY364947 in the BxPC3 tumor, can also be explained by an increase in the amount of vasculature with perfusion, not only by an increase in leakage. To test this possibility, we examined changes in perfusion by intravascular existence of dextran at only 10 min after administration, because dextran of 2 MDa should basically remain inside vasculature at that time after

doi: 10.1111/j.1349-7006.2008.01003.x

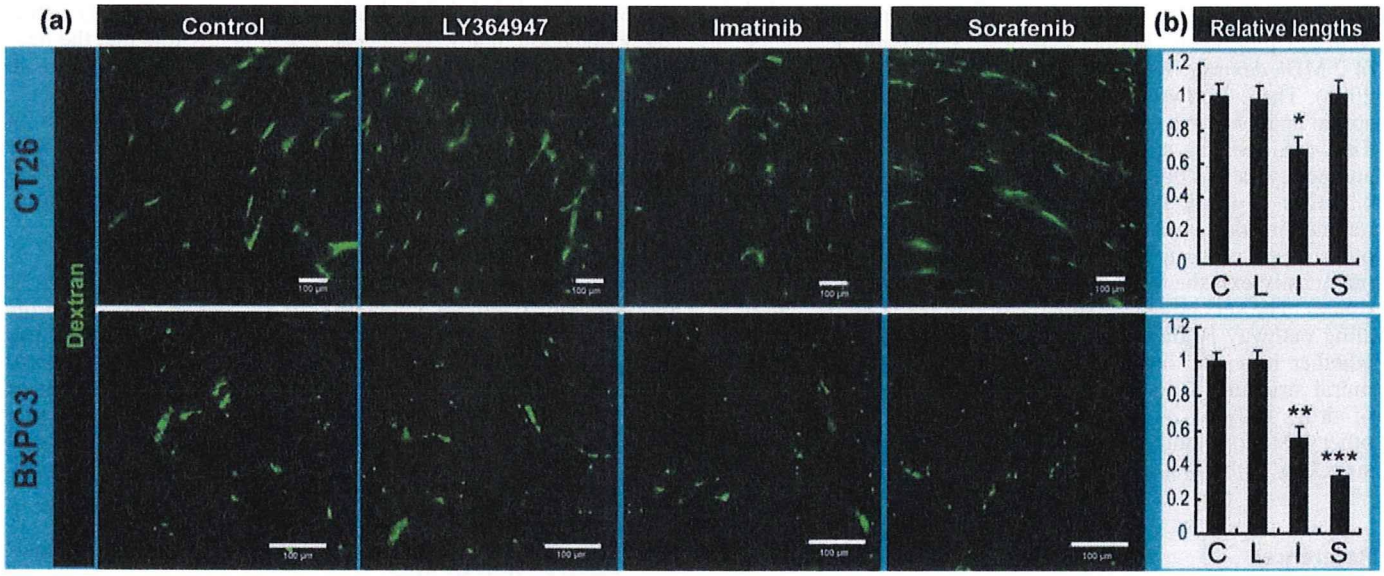

Fig. 6. Perfusion study in the tumor models. (a) Tumor vessels with perfusion were determined by the existence of dextran in green, administrated at 10 min before harvesting. Scale bars = 100 μm. (b) Relative lengths of vessels with perfusion. C, control; I, imatinib; L, LY364947; S, sorafenib. Bars represent standard errors. $*P < 0.05$; $**P < 0.01$; and $***P < 0.001$.

injection.[6] As shown in Figure 6, the lengths of vasculature with blood flow were not altered in the conditions exhibiting increased accumulation of dextran, that is, by sorafenib treatment in the CT26 tumor and by LY364947 treatment in the BxPC3 tumor. Therefore, the increased accumulation of dextran in these conditions may largely be due to an increase in vascular leakiness.

Discussion

We have previously shown that use of short-acting SMW TGF-β inhibitor can increase the distribution of nanoparticles in stroma-rich tumors by increasing the leakiness of the tumor neovasculature.[7] By virtue of the brief duration of SMWI effects, potential side effects can be decreased due to long-term suppression of essential signaling pathways. There are still a number of SMWI that can be used for manipulation of tumor neovasculature via their effects on pericytes or endothelium. We therefore compared the effects of two of these SMWI, imatinib and sorafenib.

Combined use of VEGF inhibition has been reported to have potent effects on drug delivery into tumor tissues.[19] The underlying mechanism for this has been explained by the vascular 'normalization' theory,[8] or decreased interstitial fluid pressure by decreased leakiness of tumor vasculature, via a decrease in endothelial cells and increase in pericyte coverage. Consistent with this, VEGF inhibition by sorafenib had significant effects on the retention of 2 MDa dextran in the periplug regions and in CT26 tumor, where vasculature showed less pericyte coverage and denser endothelium than in normal tissues. However, VEGF inhibition significantly decreased retention of the same dextran in adjacent areas, the intraplug region, and in BxPC3 tumor. Vascular phenotypes in these regions were characterized by more pericyte coverage and sparser endothelium, that is, they were more 'normal' than those in the periplug region and in CT26 tumor.

One of the differences between these two kinds of vasculature was the blood flow in the vasculature after sorafenib treatment. In CT26 tumor after sorafenib treatment, blood flow was maintained, whereas the flow ceased in sorafenib-treated BxPC3 tumor. These differences may partially be because of differences in sensitivity of the endothelium to the change in VEGF signaling, known to be at least due to differences in expression levels of VEGFR2.[18]

Another apparent difference in these tumor models was pericyte coverage before drug administration. Less pericyte coverage has been reported to result in more leakiness.[11–13] The degrees of dextran accumulation in all control conditions (i.e. without modification by SMWI) are consistent with the degrees of pericyte coverage. Increased dextran accumulation in LY364947-treated BxPC3 tumors can also be explained by decreased pericyte coverage, not by normalization. Both blood perfusion (Fig. 6) and interstitial fluid pressure, which we previously reported,[7] did not differ with or without LY364947 treatment in BxPC3 tumor. These findings suggest that we may need different approaches, such as the use of TGF-β inhibitor to increase drug delivery (at least for nanoparticles), to develop effective treatment for tumors with originally 'more normal' tumor vasculature. Note, however, that these more normal vessels in tumors might not be completely normal, because TGF-β inhibitor did not alter the accumulation of nanoparticles in true normal tissues, as we previously reported.[7]

Regarding the degree of original pericyte coverage in tumor vasculature, an increase in the amount of stromal components in tumor tissue may result in an increase in pericyte coverage. In a previous study, we found that the presence of FGF-2 together with VEGF-A enhances mature neovascularization compared with VEGF-A alone.[16] In addition to FGF-2, a set of signaling molecules is needed to recruit and to induce proliferation of pericytes. These include PDGF-BB[12,13] (homodimer of PDGF-B chain) and TGF-β.[11,20] These signaling molecules are reported to be secreted from components of the tumor stroma and, above all, cancer-associated fibro-blasts[21–23] and macrophages.[24] Tumors with more stroma, including fibroblasts and immune cells, have more pericyte coverage of the vasculature with greater maturity and less leakiness. Although chemoresistance of tumors has been largely investigated from the aspect of drug sensitivity of tumor cells per se, it is possible that the histological pattern of the tumor tissues may also constitute a reason for chemoresistance, because of insufficient drug delivery to the tumor cells.

The Tie2–angiopoietin signaling pathway is also known to be involved in vessel maturation and to affect pericytes.[25] Because there are no SMW compounds available to inhibit this signaling pathway, we tested the effects of one-shot Tie2-Fc chimeric

protein at 50 mg/kg bodyweight with 2 MDa dextran in the Matrigel plug assay, but no significant effects on accumulation of 2 MDa dextran were observed (M.R. Kano, unpublished data, 2008). There are two possible explanations for this observation: spatial and temporal. According to the spatial explanation, because Tie2–angiopoietin signaling occurs between the endothelium and pericytes and thus outside the vessel lumen, the Fc chimera, which is of fairly large molecular size and may therefore be retained inside vessel lumens, is not able to affect signaling. The other drugs used in the present study were all SMWI, which may easily exit the vessel lumen and penetrate the perivascular tissues. The second explanation is temporal. Although this signaling pathway is known to be deeply involved in development, whether it is also involved in the maintenance of endothelial-mural structure is not known. Because we observed the effects of drugs only at 24 h after administration, it is possible that other inhibitors inhibited only the maintenance functions of the signaling pathways, and not functions related to development. Administration of TGF-β inhibitor did not significantly affect the vasculature in normal organs,[7] so it is possible that the neovasculature requires larger amounts of signaling molecules to maintain structure than do established vessels.

In conclusion, the appropriate strategy for optimization of tumor vasculature for drug delivery system using nanoparticles may not be uniform, and may depend on tumor type, including differences in the degree of pericyte coverage of tumor vasculature.

Acknowledgments

We thank Dr Peter Baluk, Cardiovascular Research Institute, University of California, San Francisco (UCSF), for advice about perfusion. This work was supported by Grant-in-Aid for Scientific Research (KAKENHI 19790282 and 17016011) from the Ministry of Education, Culture, Sports, and Technology of Japan (MEXT), and a Health Labor Sciences Research Grant from the Ministry of Health, Labor, and Welfare of Japan.

References

1 Giroux V, Malicet C, Barthet M *et al.* p8 is a new target of gemcitabine in pancreatic cancer cells. *Clin Cancer Res* 2006; **12**: 235–41.
2 Merriman RL, Hertel LW, Schultz RM *et al.* Comparison of the antitumor activity of gemcitabine and ara-C in a panel of human breast, colon, lung and pancreatic xenograft models. *Invest New Drugs* 1996; **14**: 243–7.
3 Rothenberg ML, Moore MJ, Cripps MC *et al.* A phase II trial of gemcitabine in patients with 5-FU-refractory pancreas cancer. *Ann Oncol* 1996; **7**: 347–53.
4 Hanahan D, Weinberg RA. The hallmarks of cancer. *Cell* 2000; **100**: 57–70.
5 Jain RK. Physiological barriers to delivery of monoclonal antibodies and other macromolecules in tumors. *Cancer Res* 1990; **50**: 814S–19S.
6 Dreher MR, Liu W, Michelich CR, Dewhirst MW, Yuan F, Chilkoti A. Tumor vascular permeability, accumulation, and penetration of macromolecular drug carriers. *J Natl Cancer Inst* 2006; **98**: 335–44.
7 Kano MR, Bae Y, Iwata C *et al.* Improvement of cancer-targeting therapy, using nanocarriers for intractable solid tumors by inhibition of TGF-β signaling. *Proc Natl Acad Sci USA* 2007; **104**: 3460–5.
8 Jain RK. Normalization of tumor vasculature: an emerging concept in antiangiogenic therapy. *Science* 2005; **307**: 58–62.
9 Wilhelm S, Carter C, Lynch M *et al.* Discovery and development of sorafenib: a multikinase inhibitor for treating cancer. *Nat Rev Drug Discov* 2006; **5**: 835–44.
10 Bergers G, Song S. The role of pericytes in blood-vessel formation and maintenance. *Neuro Oncol* 2005; **7**: 452–64.
11 von Tell D, Armulik A, Betsholtz C. Pericytes and vascular stability. *Exp Cell Res* 2006; **312**: 623–9.
12 Abramsson A, Lindblom P, Betsholtz C. Endothelial and nonendothelial sources of PDGF-B regulate pericyte recruitment and influence vascular pattern formation in tumors. *J Clin Invest* 2003; **112**: 1142–51.
13 Lindblom P, Gerhardt H, Liebner S *et al.* Endothelial PDGF-B retention is required for proper investment of pericytes in the microvessel wall. *Genes Dev* 2003; **17**: 1835–40.
14 Buchdunger E, Zimmermann J, Mett H *et al.* Inhibition of the Abl protein-tyrosine kinase *in vitro* and *in vivo* by a 2-phenylaminopyrimidine derivative. *Cancer Res* 1996; **56**: 100–4.
15 Bergers G, Song S, Meyer-Morse N, Bergsland E, Hanahan D. Benefits of targeting both pericytes and endothelial cells in the tumor vasculature with kinase inhibitors. *J Clin Invest* 2003; **111**: 1287–95.
16 Kano MR, Morishita Y, Iwata C *et al.* VEGF-A and FGF-2 synergistically promote neoangiogenesis through enhancement of endogenous PDGF-B–PDGFRβ signaling. *J Cell Sci* 2005; **118**: 3759–68.
17 Vlahovic G, Rabbani ZN, Herndon JE, Dewhirst MW, Vujaskovic Z. Treatment with Imatinib in NSCLC is associated with decrease of phosphorylated PDGFR-β and VEGF expression, decrease in interstitial fluid pressure and improvement of oxygenation. *Br J Cancer* 2006; **95**: 1013–19.
18 Mancuso MR, Davis R, Norberg SM *et al.* Rapid vascular regrowth in tumors after reversal of VEGF inhibition. *J Clin Invest* 2006; **116**: 2610–21.
19 Hurwitz H, Fehrenbacher L, Novotny W *et al.* Bevacizumab plus irinotecan, fluorouracil, and leucovorin for metastatic colorectal cancer. *N Engl J Med* 2004; **350**: 2335–42.
20 Hirschi KK, Rohovsky SA, D'Amore PA. PDGF, TGF-β, and heterotypic cell–cell interactions mediate endothelial cell-induced recruitment of 10T1/2 cells and their differentiation to a smooth muscle fate. *J Cell Biol* 1998; **141**: 805–14.
21 Pietras K, Pahler J, Bergers G, Hanahan D. Functions of paracrine PDGF signaling in the proangiogenic tumor stroma revealed by pharmacological targeting. *PLoS Med* 2008; **5**: e19.
22 Micke P, Ostman A. Tumour–stroma interaction: cancer-associated fibroblasts as novel targets in anti-cancer therapy? *Lung Cancer* 2004; **45**: S163–75.
23 Bhowmick NA, Moses HL. Tumor–stroma interactions. *Curr Opin Genet Dev* 2005; **15**: 97–101.
24 Lewis CE, Pollard JW. Distinct role of macrophages in different tumor microenvironments. *Cancer Res* 2006; **66**: 605–12.
25 Armulik A, Abramsson A, Betsholtz C. Endothelial/pericyte interactions. *Circ Res* 2005; **97**: 512–23.

doi: 10.1111/j.1349-7006.2008.01003.x